IEEE Transactions on Power Delivery, Vol. 13, No. 4, October 1998

97

A NEW THEORY FOR TORSIONAL STIFFNESS OF MULTI-SPAN BUNDLE OVERHEAD TRANSMISSION LINES

Jianwei Wang **Jean-Louis Lilien**

Montefiore Electrical Institute
University of Liège, B-4000 Liège, Belgium

Abstract - A new theory for torsional stiffness of multi-span bundle overhead transmission lines is presented. The torsional mechanism is clarified. A simplified torsional stiffness formula is obtained which allows for the complex bundle stiffness to be directly calculated from the basic parameters. Applications in the choices of yoke plates and suspension clamps are detailed. The new theory correlates with experiments to a high degree of accuracy.

Keywords: Torsional Stiffness, Bundle, Galloping, Yoke Plate, Fittings.

1. INTRODUCTION

High voltage ($\geq$ 220 kV) overhead lines are generally designed as a multi-conductor arrangement per phase. The torsional behavior of such a bundle is much more complicated than that of a single conductor, which is linear and only a function of materials (aluminum, steel), its diameter and the type of strand. The bundle torsional stiffness is nonlinear and depends on the sag/span ratio, the spacer disposition and the bundle geometry, and is as well a function of the angle of rotation. The torsional stiffness is an important parameter due to its interaction with the torsional frequency, further with the flutter instability (bundle conductor galloping).

1.1 State-of-the-Art

Due to the complexity of the bundle torsional stiffness, the former theories on galloping in three-degree-of-freedom (3-DOF) [3, 7] are limited to the study of the galloping of single conductors, and fail to investigate this phenomenon for bundle conductors. Although there exist a few theories [1, 2] for bundle conductors, they are 2-DOF and only valid for small torsional movements. In 1977, Nigol *et al* [4] presented a complete model for bundle torsional stiffness (we will call this theory the *Nigol theory* in this paper), but it assumes the tension of all subconductors to be constant and equal. Another theory for bundle conductors [1] developed a new insight by taking into account tension differences between subconductors. However this theory is only valid for small rotations and neglects transversal movements. Since then, no other complete model for bundle torsional stiffness has been published until 1996, when a full multi-span 3-DOF galloping model and this new theory of torsional stiffness were presented [5]. Systematic under-estimation of the torsional stiffness in Nigol theory (especially for long spans and bundles with large number of subconductors) is the motivation to find explanations and to develop a new theory in this study. Further, the galloping mechanism is closely related to stiffness (especially to the torsional stiffness) and is thus the second reason for developing this new theory.

PE-217-PWRD-0-11-1997 A paper recommended and approved by the IEEE Transmission and Distribution Committee of the IEEE Power Engineering Society for publication in the IEEE Transactions on Power Delivery. Manuscript submitted July 21, 1997; made available for printing November 21, 1997.

1.2 Hypothesis and New Aspects

The bundle torsional stiffness is found out by an equivalent single conductor that presents similar mechanical behavior to that of a bundle of any number of subconductors. Thus, the model of torsion is limited to only one second order differential equation irrespective of the number of subconductors. Subconductors are assumed as a straight lines between two spacers.

This new theory presents the following new aspects: The physical mechanism of bundle torsional stiffness is clarified. The tension differences between subconductors are included by the connections to anchoring insulators and depend on suspension attachments. The subconductor initial angular orientation is introduced. Spacer effects are taken into account. Inter-span (within a section) interactions are also considered.

2. A NEW THEORY FOR TORSIONAL STIFFNESS

2.1 Physical Mechanism

Basically, the torsional stiffness of the overhead transmission line describes the rotational resistance of the line to the external mechanical torques applied along its longitudinal axis.

2.1.1 Single Conductor Torsional Stiffness

The torsional stiffness of a single conductor is rather constant as long as the tension remains between 10% and 35% of the ultimate tensile strength (UTS).

It increases with the size and the age of the conductor though there is no fixed relation between these variables. The increase in stiffness with the age is caused by the locking of the strands due to oxidation and creep.

The torsional stiffness can be deduced from the local torque [Nm] required to twist a stressed conductor by 1

radian, over a span length [m]. The dimension of torsional stiffness is expressed by Nm^2/rad.

The torsional stiffness of a single conductor is rather low compared to that of a bundle (about 1/20 to 1/10). The torsional stiffness of a single conductor is an intrinsic constant value (τ) for a given size and age of the conductor and is independent of the span configuration.

Referring to 87 experimental measurements performed in Belgium, Canada, France, Japan, USA, etc., τ is here given by fitting dots through both new and old (over 20 years) conductors in the log scaling as shown in Fig. 1.

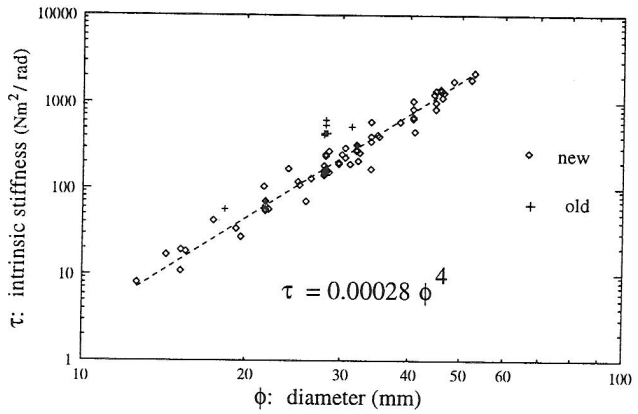

Figure 1: Measured intrinsic torsional stiffness of single conductors (typical stranded conductors with round-wire, ACSR and AAAC data are mixed in this figure.)

τ is also a function of the shape of the strand. The "smooth" conductors with trapezoidal strands present a sensibly higher intrinsic torsional stiffness. (the result of such cable is not included in Fig. 1).

From these experimental values, a good approximation of the intrinsic stiffness of the single conductor in function of its diameter is found (see Fig. 1). The exponent 4 is definitely a good choice and is logically from mathematical expression of the moment of inertia of a cylinder. It is fundamental because the exponent 4 gives a torsional ›quency independent of the conductor diameter.

2.1.2 Bundle Conductor Torsional Stiffness

The torsional stiffness of bundle conductors is highly dependent on the bundle configuration and is nonlinear for large rotations.

Generally experiments on torsional behavior of bundle conductors can be performed by either *torque-imposed* or *angle-imposed* methods. The first method is by means of a local torque applied at a constant radius of the bundle as a torsional external excitation. The response in the torsional degree of freedom is the bundle rotation angle θ. The angle-imposed method is by forcing a rotation angle, the corresponding torque is then measured by load sensors in the cable which drives the rotation angle. Fig. 2 shows the response all along the whole process of the rotation by an experimental case (the dotted parts $\overline{oabc}$, $\overline{ef}$, $\overline{gh}$ and $\overline{ij}$ are experimental results, performed by Ontario Hydro [4] using the torque-imposed method. The angle-imposed curve is qualitatively overprinted through the authors' experience).

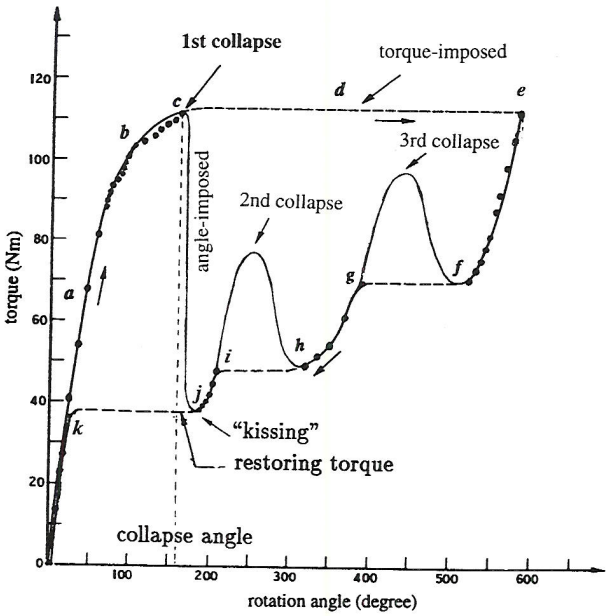

Figure 2: Physical mechanism of bundle torsional stiffness. Basic data: horizontal twin bundle, 2-span section, span length $L_1 = L_2 = 244$ m, subconductor spacing $d = 0.457$ m, 4 subspans per span. The rotation angles were obtained from the span where the torque was applied (at mid-span).

Since there is a limit to the torque which can be applied by the torque-imposed method, there exists a point (point c in this curve) where the bundle will suddenly collapse. *Collapse* means that over a given torque, the bundle rotation grows so large (static instability) that subconductors of one or several subspans will touch each other. This contact is called "kissing". After kissing, bundle stiffness is partially recovered and some other subspans (if any) will then collapse. The angle corresponding to the 1st collapse is called the *collapse angle*.

When the 1st collapse angle is reached, due to the instability a "jump" (part $\overline{cde}$) appears (by the torque-imposed method) while the 2nd and 3rd collapse (in other subspans) happen successively. Very large rotations can be observed in the whole process of collapses (more than 500 degrees in this case).

The angle-imposed method can give an access to the full curve, as shown in Fig 2, including stable (solid parts) and instable (dashed parts) stiffness branches.

Test can't be reversible by the torque-imposed method. The system will actually follow the stable branches (solid parts) and go back through $\overline{efghijk}$ with some "jumps" (dashed curves) to avoid unstable branches.

The physical torsional stiffness of bundle conductors is the tangential torsional stiffness. A negative value of tangential torsional stiffness means unstable branches. Collapse happens when the tangential torsional stiffness is zero.

Generally the value of the "restoring torque" depends on the number of subspans in contact. Full restoration is obtained at a very low torque value compared to collapse torque. This value is very much influenced by the fittings and will be detailed in the following parts of this paper.

2.2 Elastic Resultant Torque

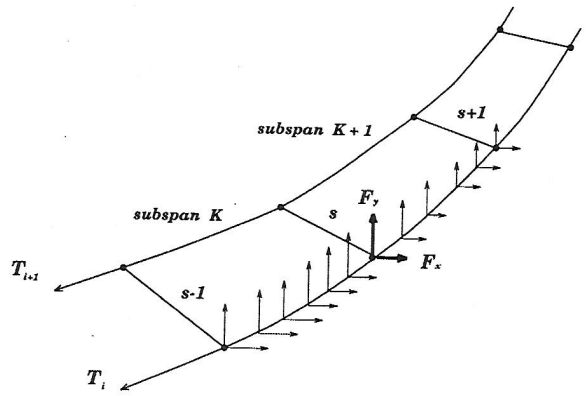

Figure 3: Distributed forces on a subconductor and located reaction forces on a spacer

Under the external excitation, there will appear a set of distributed forces along the span (see Fig. 3). Due to the bundle configurations, the torque resulting from the distributed forces can only evolve at spacer positions, in addition to the permanent contribution of the intrinsic torsional stiffness of each subconductors (which is in general a limited contribution to the global torsional stiffness and is null if spacers are with rotating clamps). The distributed forces (internal forces) are the components of the tension in each subconductor, in a plane which is perpendicular to the conductor. Elastic resultant torques are located at every spacer position, in a plane which is perpendicular to the conductor and that include the spacer itself. $C^z_{i,s}$ is the torque generated by the vertical and the transversal components of the located reaction forces (shown in Fig. 3 as F_x and F_y), that result from the integrations of the distributed forces along subspans. The global resultant torque is then the sum of all the elementary resultant torques located in each spacer plane for each subconductor:

$$C = \sum_{i=1}^{n} \sum_{s=1}^{N_s} C^z_{i,s} \tag{1}$$

where N_s is the number of subspans and n the number of subconductors.

If the bundle rotation angle θ is small, the subconductor separation is constant along each subspan but is not valid anymore for large rotations. The relative displacements between the subconductors should be taken into account. Tension differences between subconductors will then play a very important role, in relation to both their directions and magnitude. The new theory accounts for this effect and defines a new formulation of the subconductor separation.

2.3 Loads on Spacers

In practice, the multi-conductor bundles have several spacers per span. These spacers act on the torsional response of the system and their role grows bigger as the rotation becomes larger and larger. The resultant forces acting to the spacer are the reaction forces of the adjacent subspans. These forces are due to the vertical and the transversal components of the tension in the cable (see Fig. 3).

Subconductor Separation

Spacers are assumed to be weightless in this paragraph. At the *spacer location* (referring to Fig. 4 and Fig. 5), the coordinates of subconductor i are

$$\begin{cases} x_i(z) = x(z) + r\cos(\sigma_i + \theta_s) \\ y_i(z) = y(z) + r\sin(\sigma_i + \theta_s) \end{cases} \tag{2}$$

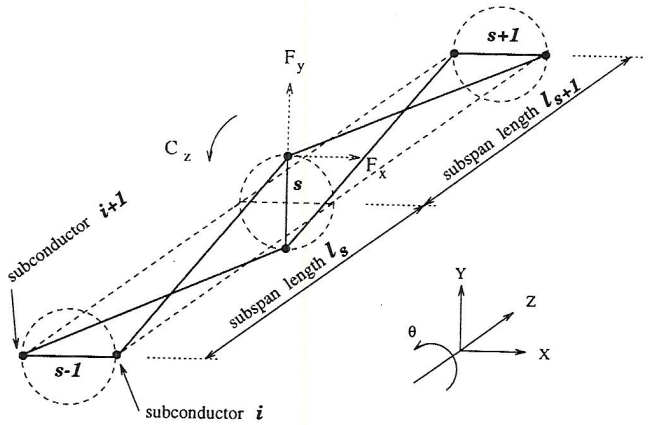

Figure 4: Schematic view of a twin bundle after a 90° differential rotation $(\theta_s - \theta_{s-1})$ between subspans

where r represents the radius of the bundle and θ_s is the angular position of spacer s (see Fig. 5). But for large rotations, the distance between subconductors all along the subspan will not remain constant. It becomes a function of z, as shown in Fig. 4 and Fig. 5. σ_i is the initial angular position of subconductor i in a bundle (e.g. $\sigma_1 = 0°$ and $\sigma_2 = 180°$ for a horizontal twin bundle). The coordinates of any point of subconductor are then:

$$\begin{cases} x_i(z) = x(z) + R(z)\cos(\sigma_i + \theta(z)) \\ y_i(z) = y(z) + R(z)\sin(\sigma_i + \theta(z)) \end{cases} \tag{3}$$

Referring to Fig. 5, the half of subconductor separation $R(z)$ is obtained [5] by

$$R(z) = r\frac{\cos\frac{\theta_{s+1} - \theta_s}{2}}{\cos(\theta - \frac{\theta_{s+1} + \theta_s}{2})} \tag{4}$$

which is used in Eq. 3. The value of R(z) can only be equal to zero when $\theta_{s+1} - \theta_s = \pi$, which means the bundle has already collapsed. But, the necessary angle of rotation for a collapse is generally lower than π.

At any point of a subconductor i, we have

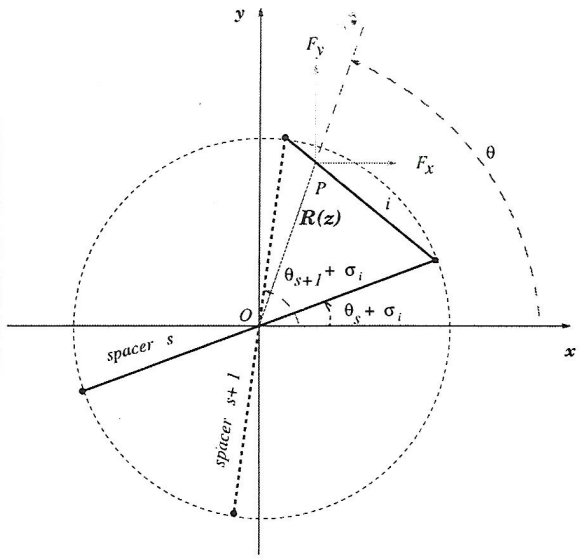

Figure 5: Subconductor separation of twin bundles

$$\begin{pmatrix} dF_x \\ dF_y \end{pmatrix} = \begin{pmatrix} d\left(T_i \dfrac{\partial x_i}{\partial z}\right) \\ d\left(T_i \dfrac{\partial y_i}{\partial z}\right) \end{pmatrix} \tag{5}$$

T_i is the subconductor tension and it depends on the stress-strain relation imposed by torsion [5], under the relation of

$$T_i = \frac{T}{n} + \Delta T_i \tag{6}$$

where T is the mean tension in the bundle. ΔT_i depends on the fitting of end towers. T_i can be considered independent of z in the actual overhead lines.

The distributed force is then given by integration along a subspan:

$$\int_{(l_s)} \begin{pmatrix} \dfrac{\partial F_x}{\partial z} \\ \dfrac{\partial F_y}{\partial z} \end{pmatrix} dz = \begin{pmatrix} \displaystyle\int_{(l_s)} T_i \frac{\partial^2 x_i}{\partial z^2} dz \\ \displaystyle\int_{(l_s)} T_i \frac{\partial^2 y_i}{\partial z^2} dz \end{pmatrix} \tag{7}$$

According to the equilibrium condition around the spacer location point, the resultant and the reaction forces can be easily computed from Eq. 7.

2.4 Torques at Spacers

For a given spacer, the distributed forces are from both adjacent subspans. The total resultant forces acting on this spacer are given by

$$\begin{cases} F_{sx} = -\dfrac{1}{l_s}\displaystyle\int_{(l_s)} T_i \frac{\partial^2 x_i}{\partial z^2} z dz \\ \qquad + \displaystyle\int_{(l_{s+1})} \left(\frac{z}{l_{s+1}} - 1\right) T_i \frac{\partial^2 x_i}{\partial z^2} dz \\ F_{sy} = -\dfrac{1}{l_s}\displaystyle\int_{(l_s)} T_i \frac{\partial^2 y_i}{\partial z^2} z dz \\ \qquad + \displaystyle\int_{(l_{s+1})} \left(\frac{z}{l_{s+1}} - 1\right) T_i \frac{\partial^2 y_i}{\partial z^2} dz \end{cases} \tag{8}$$

where $\dfrac{\partial^2 x_i}{\partial z^2}$ and $\dfrac{\partial^2 y_i}{\partial z^2}$ can be derived from Eq. 3.

Torque at the spacer s (of subconductor i) is then

$$C^z_{i,s} = F_{sy}[r\cos(\theta_s + \sigma_i)] - F_{sx}[r\sin(\theta_s + \sigma_i)] \tag{9}$$

Total torque is obtained by summing the contribution of any subspan and any subconductor (Eq. 1).

Some other contributing factors, such as the eccentric concentrated mass (called pendulum), can be easily introduced in this model [5]. This model can be easily integrated in a simulation software.

2.5 Analytical Expressions

The total torque gives an access to torsional stiffness GJ using the relation

$$\frac{\partial C}{\partial z} = GJ \frac{\partial^2 \theta}{\partial z^2} \tag{10}$$

The global expression of the torsional stiffness for small rotations can be found [5] as

$$GJ = (n\tau + r^2 T) + \frac{16r^2}{3L}\left[K_2 y_0^2 + K_1 x_0^2 - (K_3 + K_4) y_0 x_0\right] \tag{11}$$

where L is the total length of spans in the whole section. x_0 and y_0 represent initial transversal (if any) and vertical static sag. K_i depends on the flexibility matrix of anchoring (related to the yoke plate assembly, see **2.6**), the number of subconductor, bundle geometry and the sagging conditions.

The first term $(n\tau + r^2 T)$ of formula (11) is identical to Nigol theory [4] but the second one is a new term. This term can be as large as the first one so that neglecting it can lead to an under-estimation of the bundle torsional stiffness by about 50%. The second term results only from the tension differences between subconductors arising from the anchoring attachment of the bundle. The influence of this term increases as the number of spans decreases.

Considering horizontal twin bundles, we have two extreme values of torsional stiffness depending on anchoring attachments:

$$GJ_{min} = n\tau + r^2 T \tag{12}$$

$$GJ_{max} = n\tau + r^2 T + \frac{16 r^2 EA}{3L^2} y_0^2 \tag{13}$$

where E represents the Young's modulus, A the cross-section of one phase. This simplified torsional stiffness formula (13) allows for the complex bundle stiffness to be directly calculated from the basic parameters.

2.6 Effects of Yoke Plate at Anchoring Towers

In general, the yoke plate is the attachment plate which connects the subconductors to the insulators of the anchoring and suspension towers. It is a small triangular plate for a twin arrangement (see Fig. 6) and a more complex assembly for other multi-conductor bundles.

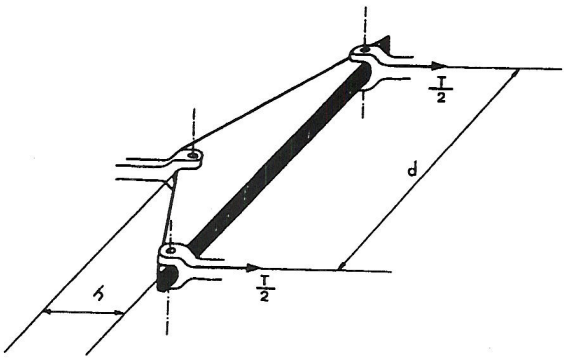

Figure 6: Twin bundle yoke arrangement, with the definition of h

The longitudinal distance (h in Fig. 6) of the yoke plate is a characteristic dimension. The anchoring assembly is described by a flexibility matrix which includes the yoke plate dimension and other parameters. The flexibility matrix of a twin bundle can be found [1] by:

$$\mathbf{F}_{twin} = \frac{d^2}{4hT}\begin{pmatrix} 1 & -1 \\ -1 & 1 \end{pmatrix} \qquad (m/N) \qquad (14)$$

This means that a small rotation of the yoke plate (in the plane defined by the conductors which are connected to it) will induce some small changes of the lengths of subconductors in the span, which induces

$$\begin{pmatrix} \Delta l_1 \\ \Delta l_2 \end{pmatrix} = \frac{d^2}{4hT}\begin{pmatrix} 1 & -1 \\ -1 & 1 \end{pmatrix}\begin{pmatrix} \Delta T_1 \\ \Delta T_2 \end{pmatrix} \qquad (15)$$

Δl_i is the span length modification of the subconductor i. Hence if $h = 0$, then $\Delta T_1 = \Delta T_2 = 0$, because Δl_i must remain finite; if $h \to \infty$, then $\Delta l_i \to 0$, because ΔT_i is finite.

For example, K_i in Eq. 11 for horizontal twin bundles can be found [5] as $K_1 = K_3 = K_4 = 0$ and

$$K_2 = (cos\sigma_1 \;\; cos\sigma_2)\left[\begin{pmatrix} \frac{2L}{EA} & 0 \\ 0 & \frac{2L}{EA} \end{pmatrix} + 2\mathbf{F}_{twin}\right]^{-1}\begin{pmatrix} cos\sigma_1 \\ cos\sigma_2 \end{pmatrix} \qquad (16)$$

where $\sigma_1 = 0°$ and $\sigma_2 = 180°$ in this case.

Regarding suspension attachments, most of the actual attachments of bundle conductors allow a free longitudinal movement between subconductors. Therefore a rotation in a span also induces a rotation in the adjacent spans. This has been taken into account in this study.

3. APPLICATIONS

3.1 The Impact of Yoke Plate Design

Table 1 shows the tension variations between subconductors which are induced by yoke plate design for a rotation of 60° at mid-span. The tension increases this amount for the subconductor going down and decreases the same amount for the subconductor going up.

Table 1: Tension differences (ΔT_i in Eq. 6) by 60° rotation for a twin bundle section of the Drake conductor with: $d = 0.457$ m, $T/2 = 35600$ N, $L = 244$ m and 4 subspans in each span.

section	$h = 0$	$h = 0.2$ m	$h = \infty$
dead-end span	0	785.3 N	1453.8 N
2-span	0	423.5 N	573.7 N
6-span	0	149.1 N	167.6 N

The characteristic dimension of yoke plate h could be considered as "infinite" if $h > 2d$ (see Fig. 7) , where d is the subconductor separation. We then get 96% of the maximum value of torsional stiffness. The curve of Fig. 7 illustrates it for a dead-end span.

Generally h/d is rather small. Some configurations present a ratio $h/d = 0.1/0.45 \approx 0.22$. It means that an increase of the yoke plate design from $h = 0.1$ m (as usual) to $h = 1.1$ m will increase the torsional stiffness of the span of about 20% ! *This can easily be achieved by installing a rigid spacer at about 1 m from the actual yoke plate attachment.*

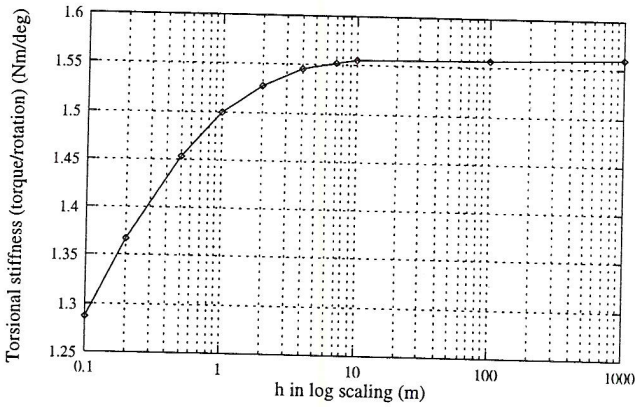

Figure 7: Torsional stiffness as a function of yoke plate design for a dead-end span of 244 m length, 0.457 m spacing, conductor diameter 28.2 mm, intrinsic stiffness 158 Nm^2/rad.

3.2 Influence of the Number of Spans and Types of Suspension Clamps

Tension differences evolve from the anchoring attachment of the bundle and also depend on the total number

of spans in a section. The higher the number of spans, the lower the torsional stiffness. The following simulation gives details on this aspect. Fig. 8 give details on the influence of the number of spans on the torsional stiffness.

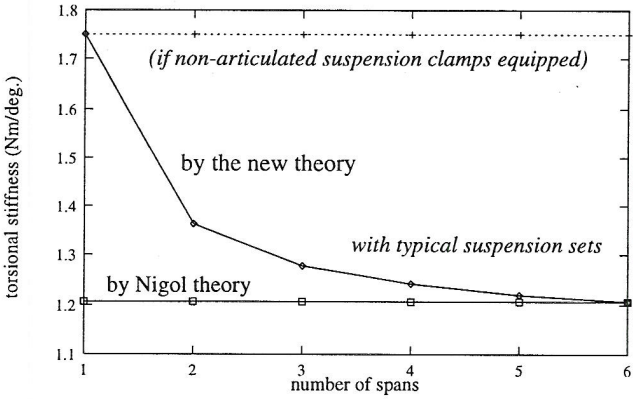

Figure 8: The influence of the number of spans on torsional stiffness (same data as used in Table 1)

From Fig. 8 it can be seen that for the same set of data, the bundle torsional stiffness of a span in a multi-span section is lower than that of a dead-end span section and depends on the number of spans in the section. In a multi-span section, the contribution of the anchoring attachment to the torsional stiffness decreases as the number of span increases. This is the reason why dead-end span sections can sometimes increase the bundle stiffness more than 50% by comparing with the same span included in a multi-span section. This is mainly because in a multi-span section, conductors can move freely and independently in longitudinal direction at the suspension clamp locations, so that tension compensates well from one span to another. Due to these reasons, *Nigol theory can only be applied to a multi-span section with a number of span higher than three and with the classical suspension attachment.*

It is possible to avoid this relative movement by non-articulated suspension clamps instead of the typical suspension clamps [6]. The number of span will not influence the torsional stiffness any more. This will shift the ratio of frequency (between vertical and torsional motions) to a significant amount. In such a case, couplings of torsional motion between spans will disappear. By this way, "up-and-down" galloping risks of bundles will disappear in most of the cases. Such new suspension set will increase the torsional stiffness by about 50% (from 1.2 Nm/deg to about 1.8 Nm/deg) and therefore induce a detuning of about 25% by shifting up the frequency of torsional motions [5, 6].

Thus, only by the change of suspension attachment, the bundle torsional stiffness of multi-span section can be easily changed.

4. COMPARISONS

4.1 Comparisons with Nigol's Results

Actually, all the experiments must remain between two extreme cases: $h = 0$ and $h = \infty$. Since the values of yoke plate have not been mentioned in the published results, two extreme cases will be presented.

Nigol *et al* gave 45 experiment cases (Fig. 9) on twin and quad bundles for a 2-span line with one suspension [4]. Fig. 9 shows a systematic under-estimation of the calculated values of the Nigol theory with respect to the experimental results, especially for long span sections and quad bundles.

Nigol's theory can be considered as a particular case for the new theory, i.e. neglecting the effects of tension differences between subconductors and this always under estimates the torsional stiffness.

Some results (two extreme values for each case) by the new theory are detailed in Fig. 10, which correlate well with the experimental values. Furthermore, long span and quad bundle cases can now be well evaluated.

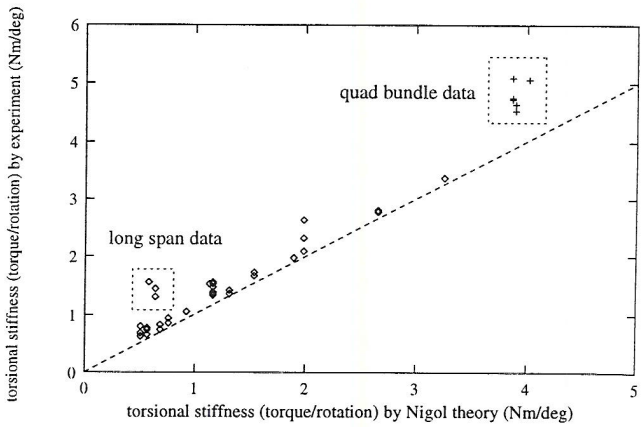

Figure 9: Torsional stiffness according to Nigol theory (extracted from [4])

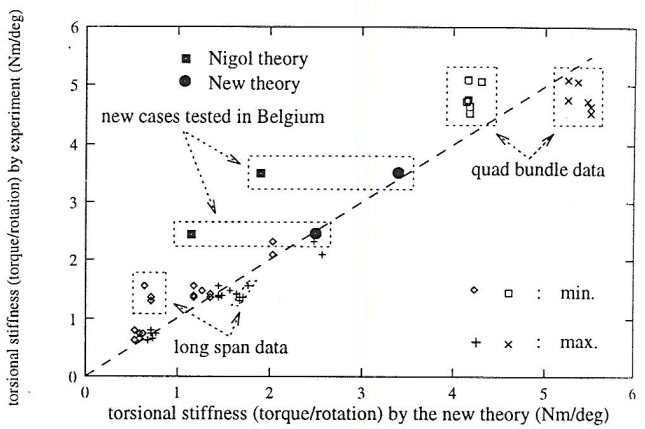

Figure 10: Torsional stiffness according to the new theory for a 2-span section. The range from the minimum ($h = 0$) to the maximum ($h = \infty$) is given for the same experimental value. Two extra cases are doted in the same figure.

4.2 Results of Full Scale Field Line

A test had been made in a dead-end span of a 380 kV transmission line by Laborelec, Belgium. The span length is 234 m. Its basic data are: AMS 2 × 620 mm^2 horizontal bundle, subconductor cross-section $A = 620$ mm^2.